Analysis of drug resistance in patient-derived renal cell carcinoma model that exhibits cancer stem-like cell traits

（がん幹細胞様特性を呈する患者由来腎がんモデルを用いた治療薬抵抗性の解析）

千葉大学大学院　医学薬学府

4年博士課程

先端医学薬学専攻（医学領域）

（主任：市川　智彦　教授）

鎌田　修平

Abstract

Background: Tyrosine kinase inhibitors (TKIs) are key therapeutic drugs for advanced renal cell carcinoma (RCC), although TKI efficacy will be often limited due to the acquired resistance, which is a critical issue in RCC management. Regarding chemoresistance, a contribution of cancer stem-like cells (CSCs) has been recently paid attention. We investigate whether cancer stemness plays a critical role in RCC cell proliferation and TKI sensitivity.

Methods: We established 15 patient-derived cancer cells (PDCs) from RCC surgical specimens and examined CSC-related gene expression and TKI sunitinib (SUN) sensitivity for each PDC line. We generated SUN-resistant RCC models from ACHN and 769-P cells.

Results: A CSC-related gene *DPP4* that encodes peptidase dipeptidyl peptidase IV is abundantly expressed in RCC among various cancers. *DPP4* expression was correlated with CSC biomarkers such as *CD133* and *ALDH1A3* in RCC PDCs. *DPP4* expression was generally associated with 50% inhibition concentration of SUN in PDCs. In SUN-resistant RCC cells, *DPP4* and *ALDH1A3* levels were upregulated compared with those in parental cells. DPP4 inhibitor sitagliptin enhanced SUN-dependent RCC growth inhibition. *DPP4* expression was repressed by ALDH1 inhibitor and recovered by retinoic acid in RCC cells. Chromatin immunoprecipitation using anti-RARα showed a functional RARα binding site in DPP4 promoter.

Conclusions: Our results define that DPP4 could be a critical factor for determining SUN sensitivity in RCC through a combinatory function of CSC biomarker ALDH1. TKI efficacy could be improved by DPP4 inhibition especially in advanced RCC with CSC enrichment.

1. Introduction

Renal cell carcinoma (RCC) is the most common tumor among kidney cancers in adults and its incidence is more than 400 ,000 worldwide in 2018[1, 2]. In general, RCC exhibits good prognosis if treated at an early stage. Nevertheless, patients with metastatic RCC are often suffered from poor prognoses despite of the usage of tyrosine kinase inhibitors such as sunitinib (SUN) or new therapeutic drugs such as immune checkpoint inhibitors. Alternative therapeutic strategies for advanced RCC remain to be established.

Clinical evidence has accumulated in terms of the relationship between metabolic disorders and cancer pathophysiology. Epidemiologic studies have revealed that type 2 diabetes is associated with an increase in incidence and mortality from solid tumors including RCC [3, 4]. Diabetic medications could potentially suppress cancer progression as exemplified by dipeptidyl peptidase 4 (DPP4) inhibitors could suppress lung metastasis of colorectal cancer [5] and tumor growth of hepatocellular carcinoma and breast cancer[6]. Metformin usage is also associated with a reduced RCC incidence among type 2 diabetic patients [7].

Recent advance in cancer studies has defined the clinical relevance of cancer stem-like cells (CSCs), which are characterized by unlimited cell division and self-renewal ability; and play an essential role in tumor recurrence, metastasis and chemoresistance [8]. CSC markers such as CD44, CD133, OCT3/4, aldehyde dehydrogenase 1 (ALDH1) and CXC-chemokine receptor 4 (CXCR4) have been also proposed as potential biomarkers for renal CSCs [9]. Among CSC markers, CD133 overexpression was observed in SUN-resistant RCC cells [10]. SUN treatment increases a subset of $CD133^{+}/CXCR4^{+}$ RCC cells, which exhibit CSC traits associated with SUN resistance[11]. DPP4/CD26 has been recently shown as a CSC-related marker in gastric [12] and colorectal cancers [13, 14]. DPP4 upregulation was also observed in high stage RCC [15] and soluble form of DPP4 was shown as a poor prognostic factor for RCC patients [16]. While a DPP4 antibody was shown to inhibit the growth of RCC cells and its xenograft tumors [17], it remains to be clarified whether DPP4 contributes to the pathophysiology of advanced RCC with CSC traits and DPP4 inhibition could facilitate RCC treatment.

In the present study, we generated 15 patient-derived cancer cells (PDCs) from surgical RCC specimens based on three-dimensional (3D) spheroid culture, which preferentially enriches CSC population [18-20]. We showed that DPP4 expression is

inversely associated with SUN sensitivity in RCC PDC lines. By establishing SUN-resistant RCC cell models, we defined a contribution of DPP4 to the growth of RCC cells and xenograft tumors. *DPP4* expression was repressed by ALDH1 inhibitor and recovered by retinoic acid (RA) in RCC cells. Chromatin immunoprecipitation (ChIP) using retinoic acid receptor α (RARα) antibody also showed a functional RARα binding site in DPP4 promoter. Taken together, CSC-related factor ALDH1 and its downstream RA/RARα signaling could potentially regulate *DPP4* transcription in RCC cells.

2. Materials and methods

2.1. Cancer cells and PDC lines

All human RCC samples were resected from patients, after obtaining an informed consent at the Saitama Medical Center. The Ethics Committee of Saitama Medical Center, Saitama Medical University, approved all the procedures performed (1363-IV). Processing of tumor samples was carried out as previously described [20]. Patients characteristics for established PDCs are summarized in Table S1.

The human RCC cell lines, ACHN and 769-P, were obtained from American Type Culture Collection (ATCC) and authenticated by short tandem repeat (STR) analysis at BEX Co., LTD (Tokyo, Japan). ACHN and 769-P cells were maintained in DMEM and RPMI medium (Nacalai Tesque, Kyoto, Japan), respectively, supplemented with 10% FBS, 100 U/ml penicillin and 100 µg/ml streptomycin at 37°C in a humidified 5% CO_2 incubator. SUN-resistant RCC cell lines, ACHN-R and 769-P-R, were generated from the parental ACHN and 769-P cells by exposure to increasing concentrations of SUN up to 10 µmol/L for more than 6 months.

2.2. Determination of the IC50 of SUN and in vitro assays for cell growth

Cells were seeded in a 96-well ultralow attachment plate at a density of 2,000 cells/well with 100 µl of medium. SUN was added at the concentrations of 0, 0.01, 0.1, 1, 2.5, 5, 7.5, 10, 12.5, 15, 20, or 50 µM. Cell growth was examined using the CellTiter-Glo 3D Assay (Promega, San Luis Obispo, CA, USA) at day 3. Average of 4 measured values were used for drawing sigmoid curves by using the ImageJ software (https://imagej.nih.gov/).

2.3. cDNA synthesis and quantitative reverse-transcription PCR

RNA extraction, cDNA synthesis and quantitative reverse-transcription (qRT)-PCR were carried out as previously described [20]. All qRT-PCR primers used in the present study are listed in Table S2.

2.4. siRNA and transfection

siRNAs targeting *DPP4* and *ALDH1A3*, and control siRNA (siControl) were purchased from RNAi Inc. (Tokyo, Japan) and introduced into cells with RNAiMAX reagents (Invitrogen, Carlsbad, CA, USA) according to the manufacturer's instructions. SiRNA sequences were listed in Table S3

2.5. Immunocytochemistry

Immunocytochemistry was carried out as described [20]. The primary antibodies used were: goat polyclonal anti-DPP4 antibody (dilution 1:100, AF1180-SP, R&D Systems, Minneapolis, MN, USA) and rabbit polyclonal anti-OCT3/4 antibody (dilution 1:100, 19857, Abcam, Cambridge, MA, USA).

2.6. Immunohistochemistry

Formalin-fixed tissues were embedded in paraffin and sectioned. The Histofine kit (Nichirei, Tokyo, Japan), which employs the streptavidin-biotin amplification method, was used for immunohistochemical analyses of DPP4. The antibodies against KI67 (dilution 1:100; MIB1) and DPP4 (dilution 1: 100, AF1180-SP) were purchased from Dako (Carpinteria, CA, USA) and R & D Systems, Inc. (Minneapolis, MN, USA), respectively. Specialized pathologists evaluated percentages of immune-positive tumor cells.

2.7. Chromatin immunoprecipitation

Chromatin immunoprecipitation (ChIP) was carried out as described previously [20]. The sequences of primers are shown in Table S4.

2.8. Animal experiments

All animal experiments were approved by the Animal Care and Use Committee of Saitama Medical University and conducted in accordance with the Guidelines and Regulations for the Care and Use of Experimental Animals by Saitama Medical University. Male athymic nude mice (BALB/c-nu/nu, 6 weeks old) were purchased from Clea Japan (Tokyo, Japan). ACHN and ACHN-R cells were trypsinized and washed with PBS, and 5×10^6 cells of each cell line were subcutaneously implanted with 150 µl Matrigel (BD Biosciences, San Diego, CA, USA). Tumor size was measured every other day. Tumor volume (V) was determined using the equation: $V = (L\times W^2)\times 0.52$, where L is the length and W is the width of the tumor. When xenografts reached a volume of 180 mm^3, the mice bearing ACHN cells were orally administered SUN (20 mg/kg), and the mice bearing ACHN-R cells were randomly selected for oral administration of either single SUN (20 mg/kg) or SUN (20 mg/kg) in combination with DPP4 inhibitor sitagliptin (SITA)(30 mg/kg). The solvent of each drug was carboxymethylcellulose sodium (0.5% wt/vol) containing NaCl (1.8% wt/vol), Tween 80 (0.4% wt/vol) and benzyl alcohol (0.9% wt/vol) as previously described [21]. Dosing schedule was 2 days on and 1 day off.

2.9. Statistical analysis

Data were analyzed with a two-sided Student's *t*-test for pairwise comparison. For multiple comparison, two-way ANOVA test was used. Statistical computations were carried out using the software JMP 9.0.0 (SAS Institute, Cary, NC, USA).

3. Results

3.1. DPP4 is highly expressed in kidney cancer PDCs.

We firstly showed that *DPP4* expression levels in kidney cancer were notably higher than those in other cancers of various origins in two datasets retrieved from Oncomine (https://www.oncomine.org/) (Fig. 1A). Next, we established kidney cancer PDCs from 15 primary tumors of clear cell RCC. The characteristics of patients corresponding to each PDCs are listed in Table S1. Furthermore, *DPP4* was upregulated in 3D cultured kidney cancer cells, ACHN and 769-P, compared to two-dimensional (2D) cultured cells. Notably, its expression was considerably higher in kidney cancer PDCs than 3D cultured ACHN and 769-P (Fig. 1B).

The 3D culture method is suitable for enrichment of CSC, therefore we evaluated the CSC population in these PDCs by immunocytochemistry for DPP4 and OCT3/4 (Fig. S1). DPP4-positive, OCT3/4-positive and double-positive rates were: 26.1%, 100% and 26.1% in RCC-9 cells; 95.7%, 95.7% and 91.3% in RCC-13 cells; 90.0%, 92.5% and 82.5% in RCC-2 cells, respectively. Hematoxylin and eosin staining and DPP4 immunohistochemistry of PDC spheroids and the corresponding original tumors showed that DPP4 staining was relatively weak in RCC-9, and strong in RCC-13 and RCC-2, in both PDCs and original tumors (Fig. 1C). Next, in 15 PDCs, we evaluated the association of *DPP4* and other CSC-related genes including, *CD133*, *ALDH1A3*, *ALDH1A1*, *OCT3/4*, *CD44*, *CXCR4* by qRT-PCR. Our results revealed that DPP4 expression levels were significantly correlated with CD133 and ALDH1A3 (Fig. S2A). *CD133* was a well-known CSC-related gene associated with SUN resistance [11, 22], hence we measured the half maximal inhibitory concentration (IC_{50}) values of SUN in PDCs. Among the genes, *CD133*, *ALDH1A3* and *DPP4* were significantly correlated with the IC_{50} values of SUN (Fig. S2B and S2C). Heatmap analysis showed the association of the expression levels of CSC-related genes and the IC_{50} values of SUN (Fig. 1D).

3.2. DPP4 was upregulated in SUN-resistant ACHN and 769-P cells

Next, we experimentally generated SUN-resistant ACHN and 769-P cells and designated them as ACHN-R and 769-P-R cells. The IC_{50} values of SUN are shown in Table 1. In SUN-resistant cells, the rates of DPP4-positive cells were increased compared to their parental cells as assessed by immunocytochemistry. DPP4-positive, OCT3/4-positive and double-positive rates were: 24.3%, 78.6% and 18.6% in ACHN cells; 68.9%, 93.4% and 65.6% in ACHN-R cells; 7.6%, 74.5% and 7.0% in 769-P cells; 94.8%, 92.9% and 90.3% in 769-P-R cells, respectively (Fig. S1). *DPP4* and *ALDH1A3* expression levels were upregulated in ACHN-R and 769-P-R (Fig. 2A and 2B).

3.3. DPP4 inhibition enhanced the growth inhibitory effect of SUN in resistant cells in vitro and in vivo

While single administration of DPP4 inhibitor SITA showed almost no effect on growth of ACHN and 769-P parental/SUN-resistant cells (Fig. S3A), the combination of SUN and SITA suppressed spheroid growth of ACHN-R/769-P-R cells, RCC-2 and

RCC-13 PDCs *in vitro* (Fig. 2C and 2D, and Fig. S3B). Moreover, DPP4 knockdown by siRNA enhanced the growth inhibitory effect of SUN in RCC-2 and RCC-13 PDCs (Fig. 3).

As *in vivo* experiment, when ACHN/ACHN-R xenograft tumor volumes reached 180 mm^3, we began oral administration of SUN with SITA and/or vehicle on schedule of 2 days on and 1 day off. ACHN-R xenograft tumors showed SUN resistance compared to parental cells, however, combination treatment of SUN and SITA suppressed tumor growth in ACHN-R tumors to the same level of ACHN with SUN (Fig. 4A-D). Ki67 immunohistochemistry and hematoxylin and eosin staining of resected tumors of representative mice in each group are shown in Fig. 4E and F. Ki67 index, a nuclear marker of cell proliferation, was elevated in ACHN-R + SUN group compared with others.

3.4. ALDH1A3 regulated DPP4 expression levels by modulating the RA and RA receptor pathway

CSC-related genes are known to be upregulated in certain situations, such as sphere forming assay and 3D culture, however the regulation of these genes remains unclear. ALDH1A3 and DPP4 have been correlated, therefore we hypothesized that there would be an association between the mechanisms of regulation of *ALDH1A3* and *DPP4*. ALDH1A3 is the enzyme involved in retinol metabolism, converting retinol to retinoic acid (RA), which acts as a ligand for RA receptors. Disulfiram, which is one of the FDA-approved inhibitors of both ALDH1 and ALDH2 used for the treatment of alcoholism, suppressed DPP4 expression levels in ACHN-R and 769-P-R cells, and this effect was reversed by the administration of all-trans retinoic acid (ATRA) (Fig. 5A). Downregulation of ALDH1A3 by siRNA also suppressed the expression levels of DPP4 (Fig. 5B). The promoter region of the *DPP4* gene that includes RARα-binding sites was retrieved from the hg38 Human Genome dataset, and scanned with matrix profiles for a RA response element (RARE) using the open-access transcription factor binding profile database JASPAR (http://jaspar.genereg.net/) [23]. At a relative profile score threshold >85% on the JASPAR algorithm, one candidate RARE was identified in about -1800 bp from the transcription start site. We confirmed functional RARα binding to the sequence including RARE in ACHN-R and 769-P-R cells by ChIP-PCR assay using a RARα

antibody or control IgG (Fig. 5C). Taken together, RA/RAR signaling may modulate *DPP4* transcription by activating the *DPP4* promoter that includes the functional RARα binding site (Fig. 5D).

4. Discussion

CSC-related genes are co-expressed under certain culture conditions, such as the 3D culture [18, 20]. However, their association with each other and their contribution to stem-like traits remain to be clarified. In the present study, the analysis of the response to SUN in CSC-enriched kidney cancer PDCs revealed that *ALDH1A3* and RA regulated the expression levels of *DPP4* via RARα binding to RARE on the promoter region, which was transcriptionally correlated with *CD133*. A previous report has shown that DPP4 is regulated by RA via phosphorylation of STAT1α [24] in B lymphocytic leukemia cells, meanwhile we demonstrated that there was direct binding of RA to the promoter region of *DPP4* in kidney cancer CSCs.

Moreover, AR had a potential role as a target for therapeutic interventions, in combination with SUN, to overcome drug resistance in RCC. Although there may be several mechanisms involved in the regulation of *DPP4*, we considered ALDH1A3/RA as one of the major pathways.

SUN is a tyrosine kinase inhibitor of platelet-derived growth factor receptors (PDGFRs) and vascular endothelial growth factor receptors (VEGFRs). DPP4 inhibitors have the potential to suppress tumor growth, because expression of VEGF was lower in Dpp4 deficient mice [25]. However, in recent studies, PDGFR-mediated anti-tumor effect has attracted attention in kidney cancer. An *in vitro* study has revealed that PDGFR-β is expressed in ACHN, Caki-1 and Caki-2 cells, and reported a tendency for a positive correlation between the sensitivity to SUN and PDGFR-β, whereas expression of VEGFR 1–3 was not observed in the three cell lines [26]. The DPP4 inhibitor SITA had the potential to attenuate PDGFR-β-induced proliferation and migration of human pulmonary arterial smooth muscle cells [27]. Regarding the association of vascularization in tumors, pre-treatment tumor fractional blood volume was found to be a predictive biomarker of subsequent reduction in tumor blood volume in response to SUN, although acquired resistance to SUN was not associated with a parallel increase in tumor blood volume [28].

While Inamoto T et al. have shown that anti-CD26 antibody treatment remarkably inhibited growth of Caki-2 RCC cells, and tumor growth in tumor-bearing mice [17], our results indicated that the DPP4 inhibitor SITA, as a single agent treatment, did not have a drastic growth inhibitory effect both on SUN-resistant cells and parental cells, whereas showed an additive effect on SUN treatment of kidney cancer CSCs. DPP4 is a serine exopeptidase that cleaves X-proline or X-alanine dipeptides from the N-terminus of polypeptides, and targets various inflammatory cytokines. IL-6 [29] and IL-8 [30] have been involved in SUN resistance, hence DPP4 may affect cytokine signaling. CXCR4, chemokine receptor 4, is also known as one of the CSC markers in RCC and there has been a report showing an association between SUN resistance and CD133 [11], however the present study did not show a positive correlation of the expression levels of *CXCR4* and SUN resistance. Adding on that, *CD44* has been reported as a CSC-related gene involved in SUN resistance [31], meanwhile has not been correlated with resistance. Further studies are required in the future to examine the interaction between CSCs and other populations of cancer cells in tumors.

ALDH1A1 and *ALDH1A3* are known to be associated with RA metabolism, whereas the expression profiles of the three subtypes of ALDH1 are different and depend on organs and tissues. Actually, it has been shown that downregulation of ALDH1A3 enhanced cisplatin sensitivity of cancer-initiating cells in lung cancer [32] and colorectal cancer cells [33], while knockdown of ALDH1A1, not ALDH1A3, reduced therapy resistance in breast cancer cells [34]. Among the three subtypes, *ALDH1A1* is one of the established CSC-related genes, and *ALDH1A2* as well as *ALDH1A3* would have essential roles in the survival of RCC PDCs. To the best of our knowledge, this is the first report to evaluate the roles of the subtypes of *ALDH1A*s in RCC. In CSC-enriched populations, *ALDH1A3* is the important subtype in tyrosine kinase inhibitor resistance.

DPP4 was notably highly expressed in RCC PDCs compared to RCC cell lines even in 3D culture conditions. Combination therapy of DPP4 inhibitors and tyrosine kinase inhibitors may be a promising treatment option for RCC patients.

5. Conclusions

Targeting of the ALDH1A3/RA/DPP4 axis is a promising treatment strategy for overcoming refractory CSC populations of renal cell carcinoma, and could be a useful tool for precision medicine.

References

[1] Siegel RL, Miller KD, Jemal A. Cancer statistics, 2018. CA Cancer J Clin 2018;68:7-30.

[2] Bray F, Ferlay J, Soerjomataram I, Siegel RL, Torre LA, Jemal A. Global cancer statistics 2018: GLOBOCAN estimates of incidence and mortality worldwide for 36 cancers in 185 countries. CA Cancer J Clin 2018;68:394-424.

[3] Bao C, Yang X, Xu W, Luo H, Xu Z, Su C, et al. Diabetes mellitus and incidence and mortality of kidney cancer: a meta-analysis. J Diabetes Complications 2013;27:357-64.

[4] Payton S. Kidney cancer: Diabetes and low serum cholesterol are risk factors for RCC. Nat Rev Urol 2014;11:422.

[5] Jang JH, Baerts L, Waumans Y, De Meester I, Yamada Y, Limani P, et al. Suppression of lung metastases by the CD26/DPP4 inhibitor Vildagliptin in mice. Clin Exp Metastasis 2015;32:677-87.

[6] Hollande C, Boussier J, Ziai J, Nozawa T, Bondet V, Phung W, et al. Inhibition of the dipeptidyl peptidase DPP4 (CD26) reveals IL-33-dependent eosinophil-mediated control of tumor growth. Nat immunol 2019;20:257-64.

[7] Tseng CH. Use of metformin and risk of kidney cancer in patients with type 2 diabetes. Eur J cancer 2016;52:19-25.

[8] Clevers H. The cancer stem cell: premises, promises and challenges. Nat Med 2011;17:313-9.

[9] Corro C, Moch H. Biomarker discovery for renal cancer stem cells. J Pathol Clin Res 2018;4:3-18.

[10] Brodaczewska KK, Bielecka ZF, Maliszewska-Olejniczak K, Szczylik C, Porta C, Bartnik E, et al. Metastatic renal cell carcinoma cells growing in 3D on polyDlysine or laminin present a stemlike phenotype and drug resistance. Oncol Rep 2019;42:1878-92.

[11] Varna M, Gapihan G, Feugeas JP, Ratajczak P, Tan S, Ferreira I, et al. Stem cells increase in numbers in perinecrotic areas in human renal cancer. Clin Cancer Res 2015;21:916-24.

[12] Nishikawa S, Konno M, Hamabe A, Hasegawa S, Kano Y, Fukusumi T, et al. Surgically resected human tumors reveal the biological significance of the gastric cancer stem cell markers CD44 and CD26. Oncol Lett 2015;9:2361-7.

[13] Cheung AH, Iyer DN, Lam CS, Ng L, Wong SKM, Lee HS, et al. Emergence of CD26+ Cancer Stem Cells with Metastatic Properties in Colorectal Carcinogenesis. Int J Mol Sci 2017;18:E1106.

[14] Grunt TW, Hebar A, Laffer S, Wagner R, Peter B, Herrmann H, et al. Prominin-1 (CD133, AC133) and dipeptidyl-peptidase IV (CD26) are indicators of infinitive growth in colon cancer cells. Am J Cancer Res 2015;5:560-74.

[15] Varona A, Blanco L, Perez I, Gil J, Irazusta J, Lopez JI, et al. Expression and activity profiles of DPP IV/CD26 and NEP/CD10 glycoproteins in the human renal cancer are tumor-type dependent. BMC Cancer 2010;10:193.

[16] Larrinaga G, Blanco L, Sanz B, Perez I, Gil J, Unda M, et al. The impact of peptidase activity on clear cell renal cell carcinoma survival. Am J Physiol Renal Physiol 2012;303:F1584-91.

[17] Inamoto T, Yamochi T, Ohnuma K, Iwata S, Kina S, Inamoto S, et al. Anti-CD26 monoclonal antibody-mediated G1-S arrest of human renal clear cell carcinoma Caki-2 is associated with retinoblastoma substrate dephosphorylation, cyclin-dependent kinase 2 reduction, p27(kip1) enhancement, and disruption of binding to the extracellular matrix. Clin Cancer Res 2006;12:3470-7.

[18] Ishiguro T, Sato A, Ohata H, Ikarashi Y, Takahashi RU, Ochiya T, et al. Establishment and Characterization of an In Vitro Model of Ovarian Cancer Stem-like Cells with an Enhanced Proliferative Capacity. Cancer Res 2016;76:150-60.

[19] Shiba S, Ikeda K, Suzuki T, Shintani D, Okamoto K, Horie-Inoue K, et al. Hormonal Regulation of Patient-Derived Endometrial Cancer Stem-like Cells Generated by Three-Dimensional Culture. Endocrinology 2019;160:1895-906.

[20] Namekawa T, Ikeda K, Horie-Inoue K, Suzuki T, Okamoto K, Ichikawa T, et al. ALDH1A1 in patient-derived bladder cancer spheroids activates retinoic acid signaling leading to TUBB3 overexpression and tumor progression. Int J Cancer

2019. doi: 10.1002/ijc.32505.

[21] Ebos JM, Lee CR, Christensen JG, Mutsaers AJ, Kerbel RS. Multiple circulating proangiogenic factors induced by sunitinib malate are tumor-independent and correlate with antitumor efficacy. Proc Natl Acad Sci U S A. 2007;104:17069-74.

[22] Luo L, Liang Y, Ding X, Ma X, Zhang G, Sun L. Significance of cyclooxygenase-2, prostaglandin E2 and CD133 levels in sunitinib-resistant renal cell carcinoma. Oncol Lett 2019;18:1442-50.

[23] Hooker TP, Hammond M, Corral K. Empyema necessitatis: review of the manifestations of thoracic actinomycosis. Cleve Clin J Med 1992;59:542-8.

[24] Bauvois B, Djavaheri-Mergny M, Rouillard D, Dumont J, Wietzerbin J. Regulation of CD26/DPPIV gene expression by interferons and retinoic acid in tumor B cells. Oncogene 2000;19:265-72.

[25] Sun CK, Leu S, Sheu JJ, Tsai TH, Sung HC, Chen YL, et al. Paradoxical impairment of angiogenesis, endothelial function and circulating number of endothelial progenitor cells in DPP4-deficient rat after critical limb ischemia. Stem Cell Res Ther 2013;4:31.

[26] Miyake M, Anai S, Fujimoto K, Ohnishi S, Kuwada M, Nakai Y, et al. 5-fluorouracil enhances the antitumor effect of sorafenib and sunitinib in a xenograft model of human renal cell carcinoma. Oncol Lett 2012;3:1195-202.

[27] Xu J, Wang J, He M, Han H, Xie W, Wang H, et al. Dipeptidyl peptidase IV (DPP-4) inhibition alleviates pulmonary arterial remodeling in experimental pulmonary hypertension. Lab Invest 2018;98:1333-46.

[28] Robinson SP, Boult JKR, Vasudev NS, Reynolds AR. Monitoring the Vascular Response and Resistance to Sunitinib in Renal Cell Carcinoma In Vivo with Susceptibility Contrast MRI. Cancer Res 2017;77:4127-34.

[29] Ishibashi K, Haber T, Breuksch I, Gebhard S, Sugino T, Kubo H, et al. Overriding TKI resistance of renal cell carcinoma by combination therapy with IL-6 receptor blockade. Oncotarget 2017;8:55230-45.

[30] Huang D, Ding Y, Zhou M, Rini BI, Petillo D, Qian CN, et al. Interleukin-8 mediates resistance to antiangiogenic agent sunitinib in renal cell carcinoma. Cancer Res 2010;70:1063-71.

[31] Mikami S, Mizuno R, Kosaka T, Saya H, Oya M, Okada Y. Expression of TNF-

alpha and CD44 is implicated in poor prognosis, cancer cell invasion, metastasis and resistance to the sunitinib treatment in clear cell renal cell carcinomas. Int J Cancer 2015;136:1504-14.

[32] Yun X, Zhang K, Wang J, Pangeni RP, Yang L, Bonner M, et al. Targeting USP22 Suppresses Tumorigenicity and Enhances Cisplatin Sensitivity Through ALDH1A3 Downregulation in Cancer-Initiating Cells from Lung Adenocarcinoma. Mol Cancer Res 2018;16:1161-71.

[33] Durinikova E, Kozovska Z, Poturnajova M, Plava J, Cierna Z, Babelova A, et al. ALDH1A3 upregulation and spontaneous metastasis formation is associated with acquired chemoresistance in colorectal cancer cells. BMC Cancer 2018;18:848.

[34] Croker AK, Rodriguez-Torres M, Xia Y, Pardhan S, Leong HS, Lewis JD, et al. Differential Functional Roles of ALDH1A1 and ALDH1A3 in Mediating Metastatic Behavior and Therapy Resistance of Human Breast Cancer Cells. Int J Mol Sci 2017;18:E2039.

Legends to figures

Fig. 1. *DPP4* is highly expressed in kidney cancer PDCs and correlated with half of the inhibitory concentration values of sunitinib. A. *DPP4* expression levels in various cancer cell lines were retrieved from the Oncomine database (https://www.oncomine.org). BLCA: bladder cancer, BCNS: brain and central nerve system tumor, BRCA: breast invasive carcinoma, COAD: colon adenocarcinoma, ESCA: Esophageal carcinoma, STAD: stomach adenocarcinoma, HNSC: head and neck squamous cell carcinoma, KC, kidney cancer, LAML: acute myeloid leukemia, LIHC: liver hepatocellular carcinoma, LC: lung cancer, LYM: lymphoma, SKCM: skin cutaneous melanoma, MYL: myeloma, OV: ovarian serous cystadenocarcinoma, PAAD: pancreatic adenocarcinoma, PRAD: prostate adenocarcinoma, SARC: sarcoma. B. *DPP4* expression levels in kidney cancer patient-derived cells (PDCs) and of two-dimensional (2D) or three-dimensional (3D) cultured ACHN and 769-P cells. C. Hematoxylin and Eosin staining, and DPP4 immunohistochemistry of PDCs and the corresponding original tumors. Bright field images of PDCs were also shown. Scale bars; 50 μm. D. Heatmaps for half maximal inhibitory concentration (IC_{50}) values of sunitinib (SUN) and mRNA expression levels of cancer stem-like cells (CSC)-related genes in PDCs.

Fig. 2. DPP4 is upregulated in sunitinib (SUN)-resistant cells and the DPP4 inhibitor sitagliptin (SITA) overcomes SUN resistance in kidney cancer cells. A and B. *DPP4* and *ALDH1A3* expression levels are upregulated in 3D cultured ACHN-R (A) and 769-P-R (B) cells compared to their parental cells. C and D. The DPP4 inhibitor sitagliptin (SITA) enhances the growth inhibitory effects of SUN on 3D cultured kidney cancer cells (C) and PDCs (D). Data are shown as mean ± SD, $n = 3$; $^*P < 0.05$ by two-sided Student's *t*-test.

Fig. 3. DPP4 knockdown by siRNA enhanced sunitinib (SUN) growth inhibitory effect in RCC-2 and RCC-13 cells. A and B. *DPP4* knockdown efficiency in RCC-2 (A) and RCC-13 (B) cells. C and D. DPP4 knockdown by siRNA enhanced SUN growth inhibitory effect in RCC-2 (C) and RCC-13 (D) cells. Data are shown as mean ± SD, $n = 3$; $^*P < 0.05$ by two-way ANOVA *t*-test.

Fig. 4. Sitagliptin (SITA) overcomes sunitinib（SUN) resistance *in vivo* tumor derived from kidney cancer cells. A. Xenograft tumor growth curve of ACHN treated by SUN and ACHN-R cells treated by SUN with/without SITA: ACHN + SU group (n = 6), ACHN-R + SUN group (n = 6) and ACHN-R + combination of SUN and SITA group (n = 6). Data are shown as mean ± SD, n = 6; *P < 0.05 by two-sided Student's t-test. The tumor volume was estimated by measuring the tumor size. B. Tumor weight and body weight at Day 13 (endpoint) in each group. Data are shown as mean ± SD, n = 6; *P < 0.05 by two-sided Student's t-test. C. Representative pictures of xenograft tumor-bearing nude mice at Day 13. Scale bars; 10 mm. D. Resected tumors from xenograft tumor-bearing nude mice at Day 13. Scale bars; 10 mm. E. Ki67 index of resected tumors. Ki67 immunohistochemistry was performed on the resected tumors and the proportion of ki67-positive cells (ki67 index) were determined. Data are shown as mean ± SD, n = 6; *P < 0.05 by two-sided Student's t-test. F. Representative images of Hematoxylin and Eosin staining, and Ki67 immunohistochemistry of resected tumors. Scale bars; 50 μm.

Fig. 5. DPP4 upregulation mediated by ALDH1A3 and retinoic acid signaling. A. All-trans retinoic acid (ATRA) rescues *DPP4* expression suppressed by the ALDH1 inhibitor disulfiram (DSF). DSF concentrations used were 15 and 25 μM for ACHN-R and 769-P-R cells, respectively. Dimethyl sulfoxide was used as vehicle. Data are shown as mean ± SD, n = 3; P-value was evaluated by two-sided Student's t-test. B. ALDH1A3 siRNA suppressed *DPP4* expression. Data are shown as mean ± SD, n = 3; P-value was evaluated by two-way ANOVA. C. RARα binding to *DPP4* promoter region. Schematic representation of *DPP4* gene promoter region with a putative retinoic acid responsive element (RARE). Chromatin immunoprecipitation (ChIP)-PCR was performed in ACHN-R and 769-P-R cells using anti-RARα antibody or control IgG. The regions containing the RARE and for background were amplified using PCR primers: Peak_Fw/Peak_Rv and Upstream_Fw/Upstream_Rv, respectively. Data are shown as mean ± SD, n = 3; P-value was evaluated by two-sided Student's t-test. D. The schematic model of ALDH1A3/RA/DPP4 axis in DPP4-high cancer stem-like cells in kidney cancer.

Table 1. IC_{50} of sunitinib (SUN) in parental and SUN-resistant cell lines

Cell lines	IC_{50} of SUN (μM)	
	2D	3D
ACHN	1.3	3.8
ACHN-R	10.0	12.9
769-P	5.0	8.8
769-P-R	12.9	12.9

Legends to Supplementary Figures

Fig. S1. Immunocytochemistry demonstrating expression of DPP4 and OCT3/4 in RCC-9, RCC-13 cells and RCC-2 PDCs. A. Immunocytochemistry of PDCs using DPP4 (green) and OCT3/4 (red) antibodies. Secondary antibodies conjugated with FITC and Cy-3 were used for detecting DPP4 and OCT3/4 antibodies, respectively. Cell nuclei were stained with DAPI (blue). B. Immunocytochemistry of 3D cultured ACHN, ACHN-R, 769-P, and 769-P-R cells using DPP4 (green) and OCT3/4 (red) antibodies. Secondary antibodies conjugated with FITC and Cy-3 were used for detecting DPP4 and OCT3/4 antibodies, respectively. Cell nuclei were stained with DAPI (blue). C. Population of DPP4-positive cells and OCT3/4-positive cells in 3D cultured RCC-9, RCC-2, RCC-13, ACHN, ACHN-R, 769-P and 769-P-R cells. DPP4-positive, OCT3/4-positive and double-positive rates: 26.1%, 100% and 26.1% in RCC-9 cells; 95.7%, 95.7% and 91.3% in RCC-13 cells; 90.0%, 92.5% and 82.5% in RCC-2 cells; 24.3%, 78.6% and 18.6% in ACHN cells; 68.9%, 93.4% and 65.6% in ACHN-R cells; 7.6%, 74.5% and 7.0% in 769-P cells; and 94.8%, 92.9% and 90.3% in 769-P-R cells. n = 5. Scale Bars; 100 μm.

Fig. S2. Correlation analysis between CSC-related gene expression levels and IC_{50} values for sunitinib (SUN) in PDCs. A. The expression levels of *DPP4* were plotted with those of CSC-related genes. B and C. The IC_{50} values for SUN were plotted against the expression levels of CSC-related genes (B) and *DPP4* (C). Spearman's rank correlation coefficient (r) and the statistical significance (p) were calculated by using JMP 9.0.0 (SAS Institute, Cary, NC, USA).

Fig. S3. DPP4 inhibition represses spheroid growth of kidney cancer cells and PDCs. A. Dose-response effect of sitagliptin (SITA) on 3D spheroid growth in ACHN-R, 769-P-R and their parental cells. B. Combination effect of SITA and sunitinib (SUN) on 3D spheroid growth of ACHN and 769-P cells. C and D. *DPP4* knockdown by siRNA enhanced the inhibitory effect of SUN on spheroid growth in RCC-2 (C) and RCC-13 (D). Data are shown as mean ± SD, n = 3; P-value was evaluated by two-sided Student's t-test.

Table S1. Characteristics of patients for renal cell carcinoma (RCC) PDCs

Name	Age	Sex	Stage	IC_{50} of SUN (μM)
RCC-1	64	M	Ⅰ	10.6
RCC-2	78	M	Ⅰ	15.3
RCC-3	67	M	Ⅲ	13.2
RCC-4	82	M	Ⅰ	5.2
RCC-5	82	M	Ⅰ	6.5
RCC-6	77	F	Ⅳ	10.8
RCC-7	56	M	Ⅰ	13.9
RCC-8	86	M	Ⅰ	11.0
RCC-9	71	M	Ⅰ	7.7
RCC-10	77	M	Ⅲ	8.0
RCC-11	80	M	Ⅰ	15.2
RCC-12	79	M	Ⅱ	7.8
RCC-13	71	M	Ⅰ	11.1
RCC-14	78	F	Ⅰ	12.2
RCC-15	83	F	Ⅰ	8.1

SUN: sunitinib, F: female, M: male.

Table S2. Sequences of primers for qRT-PCR

Primer name	Sequence
*DPP4*_Fw	CCAAACGGCACTTTTTTAGCA
*DPP4*_Rv	GAGTATTCAATAAGTGGGACTTCTGTGT
*CD44*_Fw	GTGATGGCACCCGCTATG
*CD44*_Rv	ACTGTCTTCGTCTGGGATGG
*CD133*_Fw	CAGAGTACAAACGCCAAACCA
*CD133*_Rv	AAATCACGATGAGGGTCAGC
*OCT3/4*_Fw	TTCAGCCAAACGACCATCTG
*OCT3/4*_Rv	CACGAGGGTTTCTGCTTTGC
*ALDH1A1*_Fw	CGCAAGACAGGCTTTTCAGAT
*ALDH1A1*_Rv	CCCTCTCGGAAGCATCCA
*ALDH1A3*_Fw	TGGATCAACTGCTACAACGC
*ALDH1A3*_Rv	CACTTCTGTGTATTCGGCCA
*CXCR4*_Fw	GCATGACGGACAAGTACAGGCT
*CXCR4*_Rv	AAAGTACCAGTTTGCCACGGC
*36B4*_Fw	CCACGCTGCTGAACATGCT
*36B4*_Rv	GATGCTGCCATTGTCGAACA

Table S3. Sequences of small interfering RNAs for knockdown of target genes

Oligo nucleotide name		Sequence
siDPP4 #1	Sense strand	GGAGGGUACGUAACCUCAAUG
	Antisense strand	UUGAGGUUACGUACCCUCCAU
siDPP4 #2	Sense strand	CAGUCGCAAAACUUACACUCU
	Antisense strand	AGUGUAAGUUUUGCGACUGUC
siALDH1A3 #1	Sense strand	UUUUGAACUUCAGUAUUGGUU
	Antisense strand	CCAAUACUGAAGUUCAAAAGU
siALDH1A3 #2	Sense strand	UUUUCACUUCUGUGUAUUCGG
	Antisense strand	GAAUACACAGAAGUGAAAACU
siControl	Sense strand	GUACCGCACGUCAUUCGUAUC
	Antisense strand	UACGAAUGACGUGCGGUACGU

Table S4. Sequences of primers for ChIP-PCR

Primer name	Sequence
Peak_Fw	CTAATGTGTTGGCCAGCTGCTACC
Peak_Rv	GTCCGATGGGGCATTACCACATGA
Upstream_Fw	GTCCAGGCTGAGGTGGTCTCATGC
Upstream_Rv	TGGCAAGAGTCACCACTGCTCCAG

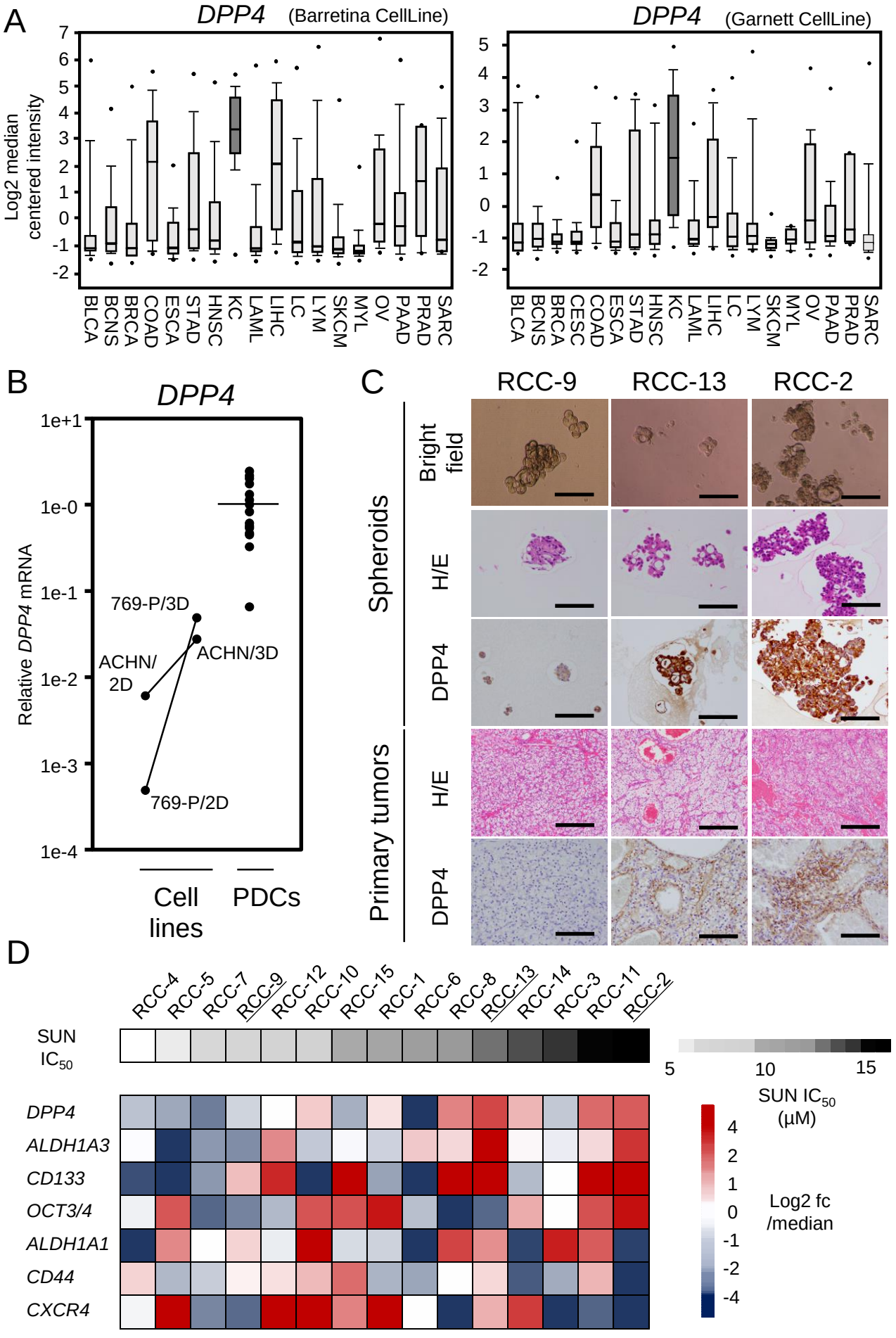
A
DPP4 (Barretina CellLine)
DPP4 (Garnett CellLine)
Log2 median centered intensity
BLCA BCNS BRCA COAD ESCA STAD HNSC KC LAML LIHC LC LYM SKCM MYL OV PAAD PRAD SARC
BLCA BCNS BRCA CESC COAD ESCA STAD HNSC KC LAML LIHC LC LYM SKCM MYL OV PAAD PRAD SARC
B
DPP4
Relative DPP4 mRNA
769-P/3D
ACHN/3D
ACHN/2D
769-P/2D
Cell lines
PDCs
C
RCC-9
RCC-13
RCC-2
Spheroids
Primary tumors
Bright field
H/E
DPP4
H/E
DPP4
D
RCC-4 RCC-5 RCC-7 RCC-9 RCC-12 RCC-10 RCC-15 RCC-1 RCC-6 RCC-8 RCC-13 RCC-14 RCC-3 RCC-11 RCC-2
SUN IC50
SUN IC50 (μM)
DPP4
ALDH1A3
CD133
OCT3/4
ALDH1A1
CD44
CXCR4
Log2 fc /median

Fig. 1.

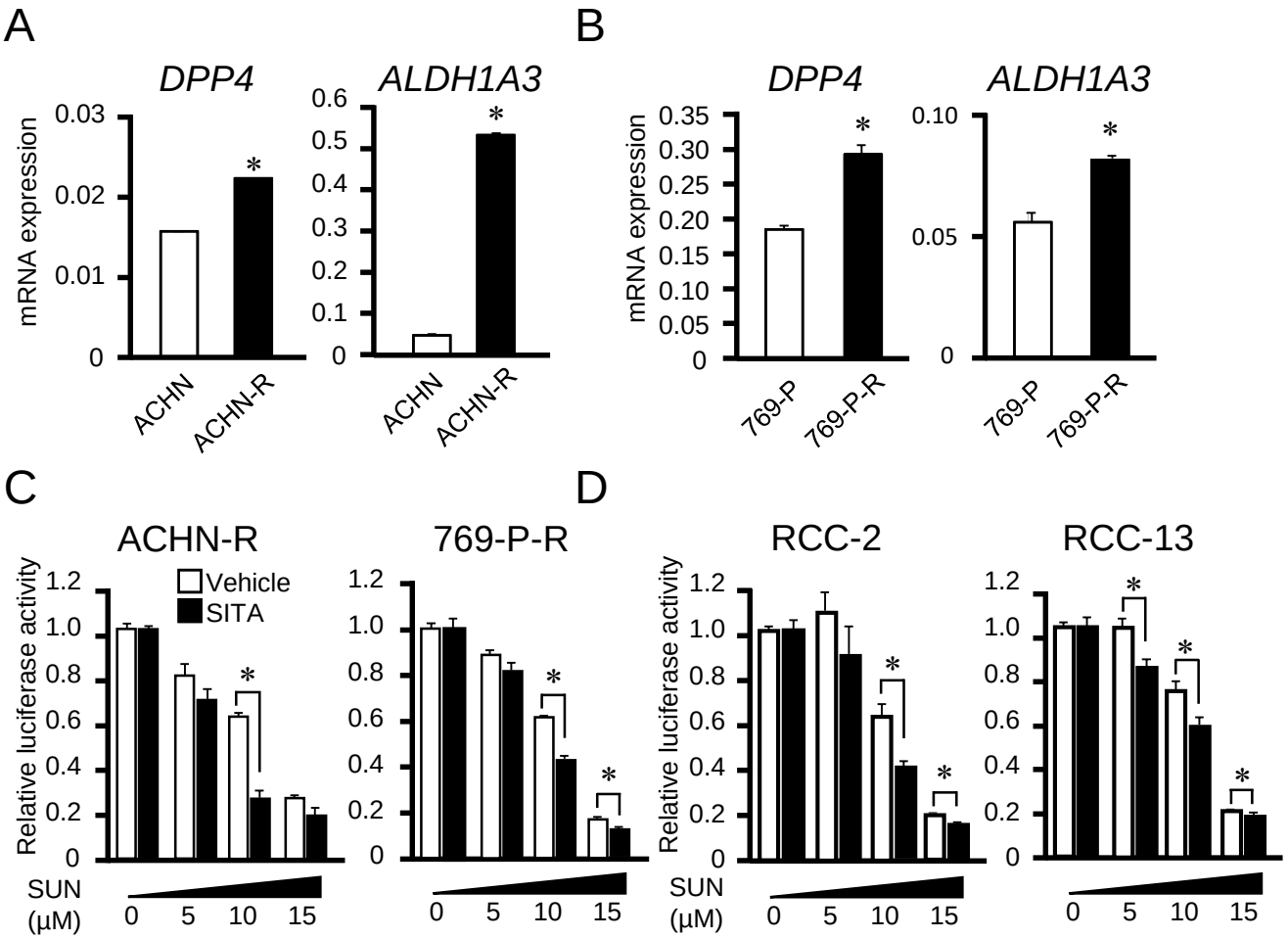
A
DPP4
ALDH1A3
mRNA expression
0.03
0.02
0.01
0
0.6
0.5
0.4
0.3
0.2
0.1
0
*
*
ACHN
ACHN-R
ACHN
ACHN-R
B
DPP4
ALDH1A3
mRNA expression
0.35
0.30
0.25
0.20
0.15
0.10
0.05
0
0.10
0.05
0
*
*
769-P
769-P-R
769-P
769-P-R
C
ACHN-R
769-P-R
Vehicle
SITA
Relative luciferase activity
1.2
1.0
0.8
0.6
0.4
0.2
0
*
*
*
*
SUN
(μM)
0
5
10
15
0
5
10
15
D
RCC-2
RCC-13
Relative luciferase activity
1.2
1.0
0.8
0.6
0.4
0.2
0
*
*
*
*
*
*
SUN
(μM)
0
5
10
15
0
5
10
15

Fig. 2.

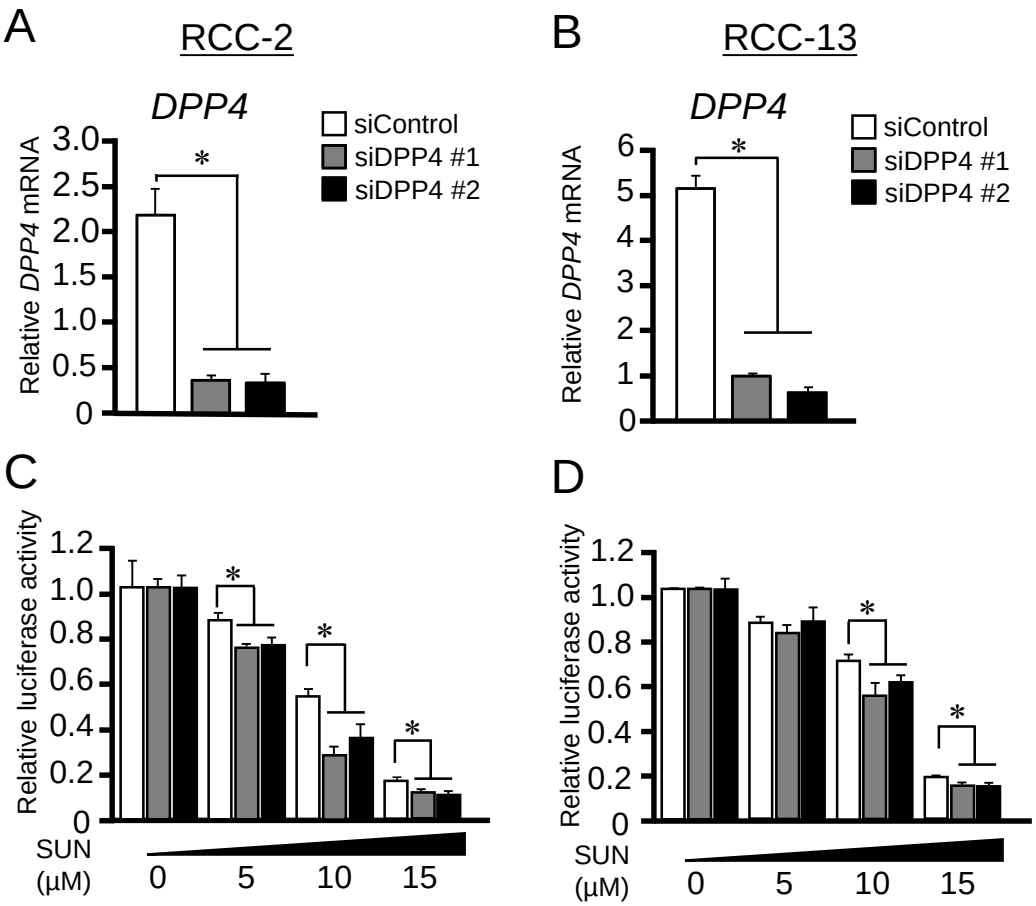
A
RCC-2
DPP4
siControl
siDPP4 #1
siDPP4 #2
Relative DPP4 mRNA
3.0
2.5
2.0
1.5
1.0
0.5
0
*
B
RCC-13
DPP4
siControl
siDPP4 #1
siDPP4 #2
Relative DPP4 mRNA
6
5
4
3
2
1
0
*
C
Relative luciferase activity
1.2
1.0
0.8
0.6
0.4
0.2
0
*
*
*
SUN
(μM)
0
5
10
15
D
Relative luciferase activity
1.2
1.0
0.8
0.6
0.4
0.2
0
*
*
SUN
(μM)
0
5
10
15

Fig. 3.

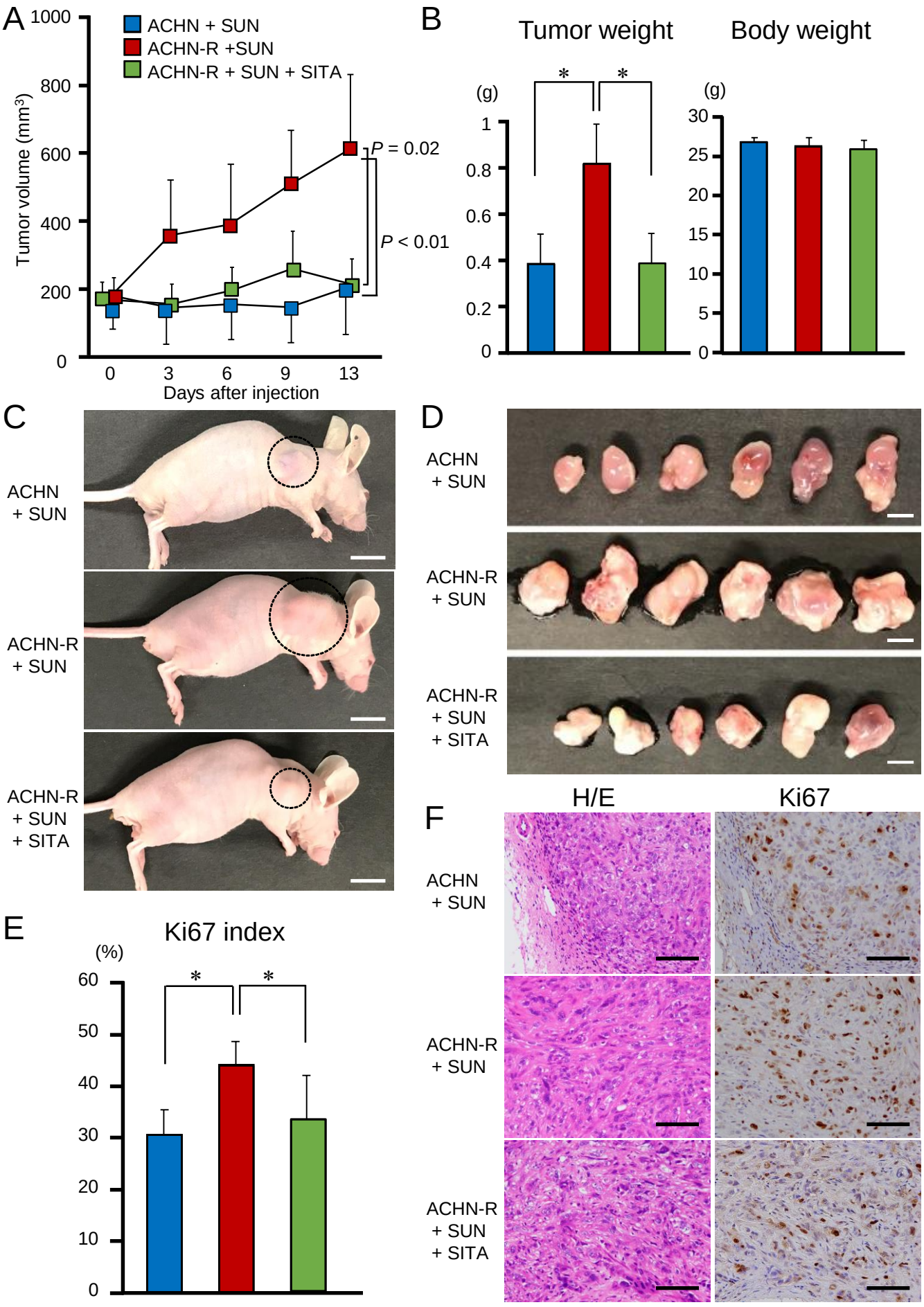
A
ACHN + SUN
ACHN-R +SUN
ACHN-R + SUN + SITA
Tumor volume (mm3)
1000
800
600
400
200
0
0
3
6
9
13
Days after injection
P = 0.02
P < 0.01
B
Tumor weight
Body weight
(g)
1
0.8
0.6
0.4
0.2
0
30
25
20
15
10
5
0
C
ACHN + SUN
ACHN-R + SUN
ACHN-R + SUN + SITA
D
ACHN + SUN
ACHN-R + SUN
ACHN-R + SUN + SITA
E
Ki67 index
(%)
60
50
40
30
20
10
0
F
H/E
Ki67
ACHN + SUN
ACHN-R + SUN
ACHN-R + SUN + SITA

Fig. 4.

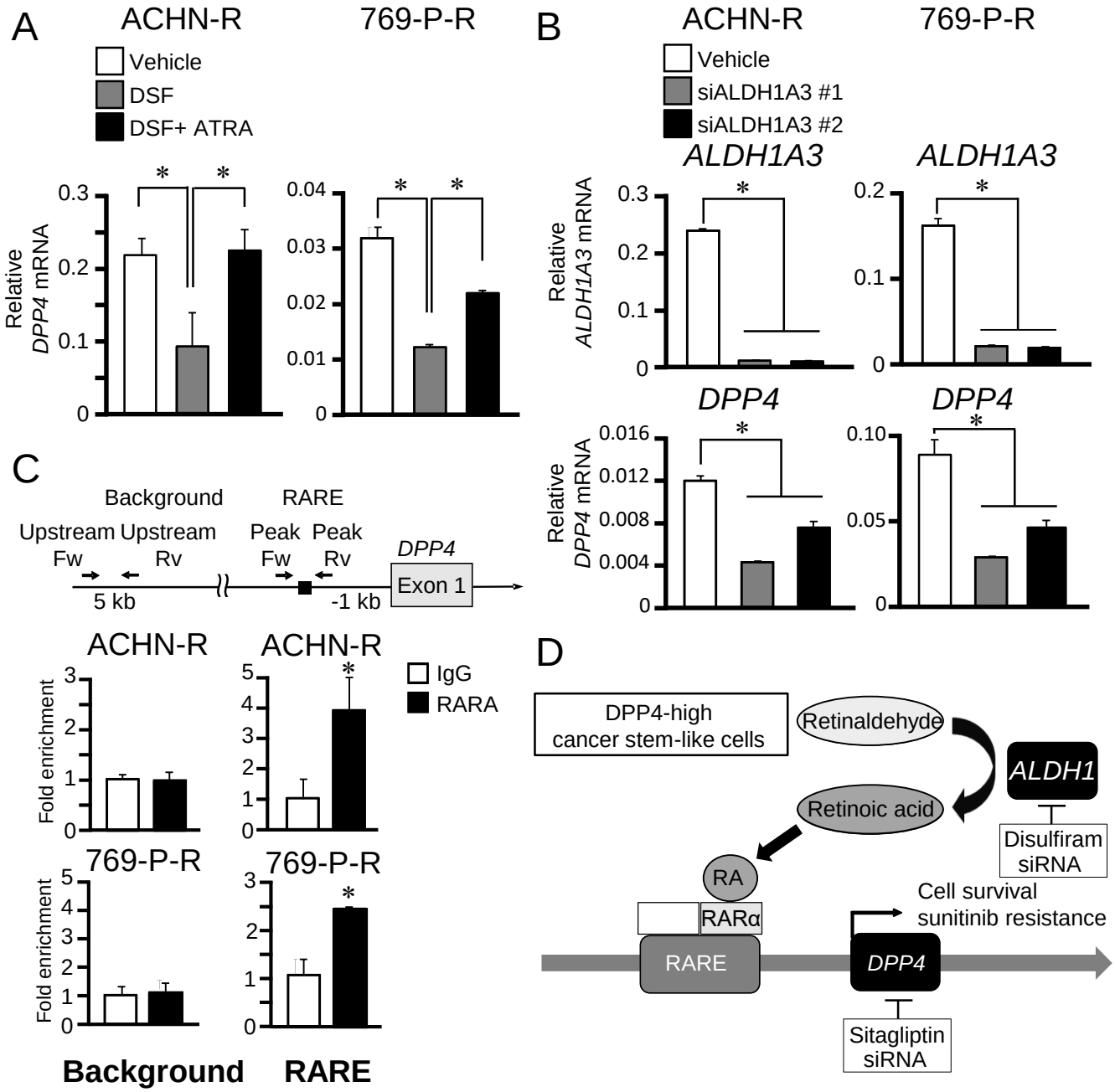
A
ACHN-R
769-P-R
Vehicle
DSF
DSF+ ATRA
Relative DPP4 mRNA
B
ACHN-R
769-P-R
Vehicle
siALDH1A3 #1
siALDH1A3 #2
ALDH1A3
ALDH1A3
Relative ALDH1A3 mRNA
DPP4
DPP4
Relative DPP4 mRNA
C
Background
RARE
Upstream Fw
Upstream Rv
Peak Fw
Peak Rv
DPP4
Exon 1
5 kb
-1 kb
ACHN-R
ACHN-R
IgG
RARA
Fold enrichment
769-P-R
769-P-R
Fold enrichment
Background
RARE
D
DPP4-high cancer stem-like cells
Retinaldehyde
ALDH1
Retinoic acid
Disulfiram siRNA
RA
RARα
Cell survival sunitinib resistance
RARE
DPP4
Sitagliptin siRNA

Fig. 5.